ARTICLE

Detection and characterization of serine and threonine hydroxyl protons in *Bacillus circulans* xylanase by NMR spectroscopy

Jacob A. Brockerman · Mark Okon ·
Lawrence P. McIntosh

Abstract Hydroxyl protons on serine and threonine residues are not well characterized in protein structures determined by both NMR spectroscopy and X-ray crystallography. In the case of NMR spectroscopy, this is in large part because hydroxyl proton signals are usually hidden under crowded regions of ^{1}H-NMR spectra and remain undetected by conventional heteronuclear correlation approaches that rely on strong one-bond ^{1}H–^{15}N or ^{1}H–^{13}C couplings. However, by filtering against protons directly bonded to ^{13}C or ^{15}N nuclei, signals from slowly-exchanging hydroxyls can be observed in the ^{1}H-NMR spectrum of a uniformly ^{13}C/^{15}N-labeled protein. Here we demonstrate the use of a simple selective labeling scheme in combination with long-range heteronuclear scalar correlation experiments as an easy and relatively inexpensive way to detect and assign these hydroxyl proton signals. Using auxtrophic *Escherichia coli* strains, we produced *Bacillus circulans* xylanase (BcX) labeled with ^{13}C/^{15}N-serine or ^{13}C/^{15}N-threonine. Signals from two serine and three threonine hydroxyls in these protein samples were readily observed via $^3J_{C-OH}$ couplings in long-range ^{13}C-HSQC spectra. These scalar couplings ($\sim$5–7 Hz) were measured in a sample of uniformly ^{13}C/^{15}N-labeled BcX using a quantitative ^{13}C/^{15}N-filtered spin-echo difference experiment. In a similar approach, the threonine and serine hydroxyl hydrogen exchange kinetics were measured using a ^{13}C/^{15}N-filtered CLEANEX-PM pulse sequence. Collectively, these experiments provide insights into the structural and dynamic properties of several serine and threonine hydroxyls within this model protein.

Keywords Glycoside hydrolase · Hydroxyl amino acid · Protein structure and dynamics · NMR spectroscopy

J. A. Brockerman · M. Okon · L. P. McIntosh (✉)
Department of Biochemistry and Molecular Biology, Life Sciences Centre, University of British Columbia, 2350 Health Sciences Mall, Vancouver, BC V6T 1Z3, Canada
e-mail: mcintosh@chem.ubc.ca

J. A. Brockerman · M. Okon · L. P. McIntosh
Department of Chemistry, and Michael Smith Laboratories, University of British Columbia, Vancouver, BC V6T 1Z3, Canada

Introduction

Serine and threonine residues often play key structural and functional roles in proteins due to their sidechain hydroxyls serving as hydrogen bond donors/acceptors (Creighton 2010). However, unless neutron (Kossiakoff et al. 1990) or very high resolution X-ray diffraction (Ho and Agard 2008) data are available, the positions of hydroxyl protons are most often inferred, rather than directly observed, in crystallographically-determined structures of proteins. Similarly, only $\sim$1 % of the NMR spectral assignments reported for serine and threonine residues in the BioMagResBank correspond to hydroxyl protons. Several factors have contributed to this under-representation, including the generally rapid exchange of these labile protons (Liepinsh et al. 1992; Liepinsh and Otting 1996) and the lack of any one-bond scalar couplings with neighbouring spin-1/2 nuclei. Indeed, most current NMR methods for studying proteins rely upon ^{15}N- or ^{13}C-based heteronuclear approaches, and thus signals from slowly exchanging serine ^{1}H$^\gamma$ and threonine ^{1}H$^{\gamma1}$ hydroxyl protons will not be readily detected. Furthermore, with average chemical shifts of 5.47 ± 1.1 and 5.19 ± 1.2 ppm, respectively (Ulrich et al.

2008), their signals will usually be buried under the envelope of water and protein peaks in crowded ^{1}H-NMR spectra. Accordingly, the limited number of hydroxyl assignments reported to date have been derived mainly from potentially ambiguous through-space ^{1}H–^{1}H NOE interactions, and to a lesser extent, via $^3J_{H\beta-OH}$ couplings detected in scalar correlation spectra (Liepinsh et al. 1992; Knauf et al. 1993; Peelen and Vervoort 1994; Takeda et al. 2011). It is noteworthy that hydroxyl signals have also been observed due to scalar couplings across OH⋯OP hydrogen bonds in ^{31}P-HMQC spectra of a flavoprotein (Lohr et al. 2000), as well as in dipolar-based solid state NMR spectra of a deuterated microcrystalline SH3 domain (Agarwal et al. 2010).

The goal of this study was to further develop NMR spectroscopic methods for detecting and unambiguously assigning the signals from serine and threonine hydroxyls in proteins. As a model system, we focused on the well characterize 20 kDa xylanase from *Bacillus circulans* (BcX). When the 1D ^{1}H-NMR spectrum of the uniformly ^{13}C/^{15}N-labeled protein is recorded with filtering against protons directly bonded to ^{13}C or ^{15}N nuclei, numerous signals are still detected (Fig. 1). These most likely arise from slowly exchanging hydroxyl groups as BcX lacks any cysteines and, with the exception of the catalytic general acid Glu172, all carboxyl moieties are deprotonated under the experimental conditions of pH 6 (McIntosh et al. 2011). The most downfield of the OH signals were assigned previously to 4 of the 15 tyrosines in BcX via three-bond ^{1}H$^\eta$–^{13}C$^\varepsilon$ couplings detected in a long-range ^{13}C-HSQC spectrum (Baturin et al. 2011). Thus, we speculated that many of the remaining signals arose from some of the 18 serines and 25 threonines present in this protein. Using a combination of amino acid selective isotopic labeling and long-range ^{13}C-HSQC experiments, we confirmed this hypothesis and assigned the signals from two serine and three threonine hydroxyl protons. These assignments enabled structural and dynamic studies of BcX through $^3J_{C-OH}$ scalar coupling and hydrogen exchange (HX) measurements, respectively.

Materials and methods

Protein expression and purification

The expression and purification of BcX followed previously described protocols (Sung et al. 1993; Joshi et al. 2001). Briefly, uniformly ^{13}C/^{15}N-labeled BcX was produced in prototrophic *Escherichia coli* BL21 (λDE3) cells transformed with a pET22b(+) vector encoding the enzyme. The cells were grown in LB media at 37 °C to an OD$_{600}$ of ∼0.6, pelleted via gentle centrifugation, and resuspended in M9 media containing 1 g/L 98 % ^{15}NH$_4$Cl
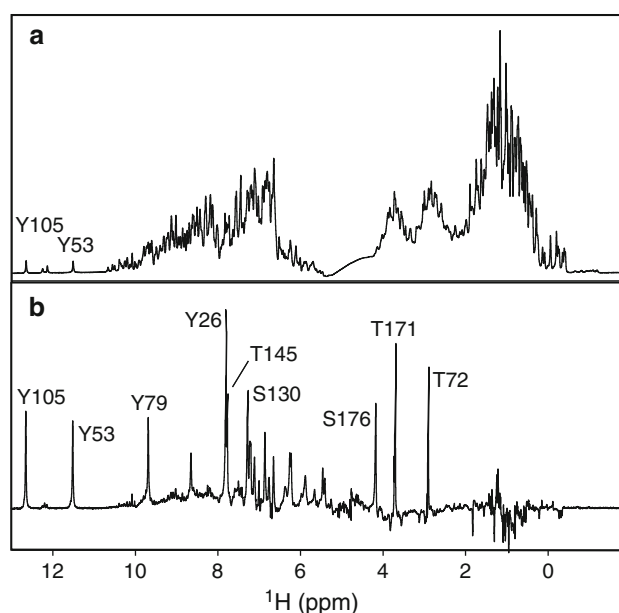

Fig. 1 a The ^{1}H-NMR spectrum of uniformly ^{13}C/^{15}N-labeled BcX recorded without ^{13}C/^{15}N-decoupling. Downfield of amide envelope are apparent singlets arising from two tyrosine O$^\eta$H protons and a doublet at 12.2 ppm from the ^{15}N-bonded ^{1}H$^{\varepsilon 2}$ of His149 (Plesniak et al. 1996a; Baturin et al. 2011). **b** The ^{13}C/^{15}N-filtered spectrum of ^{13}C/^{15}N-BcX reveals many additional ^{1}H signals originating from oxygen-bonded protons, five of which were assigned in this study. Weak noisy peaks, such as those in the methyl region, arise from incomplete filtering. The spectra were recorded at pH 6 and 25 °C (850 MHz spectrometer) using the pulse sequence in Supplemental Fig. S5. This sequence exploits two different spin echo delays to filter signals from ^{1}H–^{13}C pairs with a wide range of $^1J_{CH}$ values (Ogura et al. 1996; Zwahlen et al. 1997; Breeze 2000; Iwahara et al. 2001), and a WATERGATE approach to dephase the signal from water (Piotto et al. 1992)

and 3 g/L 99 % ^{13}C$_6$-glucose. After 45 min at 30 °C, BcX expression was induced with 0.1 mM IPTG.

BcX samples selectively labeled with ^{13}C/^{15}N-serine or -threonine were produced using *E. coli* JC158 or JW0003-2 cells, respectively. The auxotrophic cells were obtained from the Yale Coli Genetic Stock Centre, transformed with a pCW–BcX vector, and grown in an artificial rich medium containing 0.5 g/L of [^{13}C$_3$/^{15}N]-L-serine (Sigma-Aldrich) or 0.12 g/L of [^{13}C$_4$/^{15}N]-L-threonine (Sigma-Aldrich), along with all other unlabeled amino acids (Muchmore et al. 1989). In each case, the auxotrophic *E. coli* cells were grown at 37 °C to OD$_{600}$ ∼0.6 in LB media, pelleted by gentle centrifugation, and resuspended in the medium lacking either serine or threonine. After growth for 45 min at 30 °C, the labeled amino acid was added and protein expression induced with 1 mM IPTG.

Four to 6 h post-induction, the cells were harvested by centrifugation and lysed by sonication in the presence of a protease inhibitor cocktail (Roche Diagnostics). The resulting BcX samples were purified using an SP-Sepharose ion exchange column (GE Healthcare) with a 0–1 M

NaCl gradient in 10 mM sodium phosphate buffer, pH 6, followed by gel filtration on a HiPrep 16/60 Sphacryl S-100 size exclusion column (GE Healthcare) equilibrated with 10 mM sodium phosphate buffer, pH 6. The final samples were concentrated to ~ 0.6 mM in the latter buffer via ultrafiltration with a 10 KD MWCO Amicon Ultra centrifugal filter, and 5 % D_2O was added as a lock solvent.

Protein characterization

Escherichia coli JW0003-2 (F-, $\Delta thrC724$::kan, $\Delta(araD-araB)567$, $\Delta lacZ4787$(::rrnB-3), λ^-, rph-1, $\Delta(rhaD-rhaB)568$, hsdR514) from the Keio collection (Baba et al. 2006) is a well-behaved threonine auxotroph. The resulting BcX was selectively $^{13}C/^{15}N$-labeled at only these residues, as verified by ^{13}C- and ^{15}N-HSQC spectra (Supplemental Fig. S1). In contrast, *E. coli* JC158 (lacI22, λ^-, e14-, relA1, serA6, spoT1, thiE1) (Clark 1963) is a leaky serine auxotroph, presumably using glycine as a metabolic precursor (Waugh 1996). Although not quantitated, the resulting BcX appeared only partially enriched in $^{13}C/^{15}N$-serine based on relative ^{13}C- and ^{15}N-HSQC spectral intensities. Also, due to metabolic interconversion, some ^{15}N-labeling of the alanine, tryptophan and glycine amides (~ 2, 9 and 12 % relative ^{15}N-HSQC peak intensities vs those of the serine amides, respectively) and ^{13}C-labeling of the alanine methyls occurred (Supplemental Fig. S2). It is noteworthy that in preliminary experiments carried out with prototrophic *E. coli* BL21, significant metabolic interconversion of both ^{15}N-threonine and ^{15}N-serine occurred as evidenced by the ^{15}N-HSQC spectra of the resulting proteins (Supplemental Fig. S3). Thus, the advantages of using auxotrophic *E. coli* strains include increased labeling selectivity and minimization of the amount of labeled amino acid necessary to ensure adequate bacterial growth and protein expression (Muchmore et al. 1989).

NMR spectroscopy

NMR spectra were recorded at 25 °C with Bruker Avance III 500, 600, and 850 MHz spectrometers equipped with xyz-gradient TCI cryoprobes. Data were processed with NMRpipe (Delaglio et al. 1995), and analyzed using Sparky (Goddard and Kneeler 1999) and Topspin. Signals from the serine and threonine non-hydroxyl ^1H, ^{13}C, and ^{15}N nuclei were assigned based on the previously reported spectra of BcX (Plesniak et al. 1996b; Connelly et al. 2000) and confirmed using *intra*-residue H(C)TOCSY-NH and C(C)TOCSY-NH spectra recorded with the $^{13}C/^{15}N$-serine or -threonine labeled proteins (Supplemental Fig. S4). These spectra differed from the more commonly used inter-residue versions as the amides following the serines and threonines were unlabeled. Signals from the serine and threonine hydroxyls were characterized

with a variety of single- and multiple-bond (long-range) correlation experiments, presented in the "Results" section. Details of most pulse sequences used in this study are documented as Supplemental Figs. S5-S12.

$^3J_{C-OH}$ quantitation

Three-bond scalar couplings for the detected hydroxyls were measured using a quantitative spin-echo difference experiment with a $^{13}C/^{15}N$-filtered readout (Supplemental Fig. S9). The data were recorded for uniformly $^{13}C/^{15}N$-labeled BcX at pH 6.0 and 25 °C using an 850 MHz spectrometer. Difference (I_{diff}) and reference (I_{ref}) peak heights were measured with spin echo Δ delay periods of 21 ms, and used to solve for $^3J_{C-OH}$ according to the equation (Blake et al. 1992)

$$I_{diff}/I_{ref} = 1 - \cos(2\pi/^3J_{C-OH}\Delta)$$

The reported $^3J_{C-OH}$ are the average values from data recorded with either a broadband ^{13}C inversion pulse or on-resonance hard pulses during the final spin echo of the pulse sequence.

Hydrogen exchange kinetics

Hydroxyl HX kinetics were measured using a 1D CLEANEX-PM experiment (Hwang et al. 1997) with a $^{13}C/^{15}N$-filtered readout (Supplemental Fig. S10). The data were recorded for uniformly $^{13}C/^{15}N$-labeled BcX at pH 6.0 and 25 °C using a 600 MHz spectrometer. Peak heights (I_i) were measured as a function of transfer time (t_i), and fit with Mathworks Matlab to the equation,

$$\frac{I_i}{I_o} = \left(\frac{k_{ex}}{k_{ex} + R_{app}}\right)\left(1 - e^{-(k_{ex}+R_{app})t_i}\right)$$

where I_o is the corresponding signal height in a control spectrum recorded without exchange, k_{ex} is the exchange rate constant, and R_{app} is an apparent rate constant due to both transverse and longitudinal relaxation. Recycle delays were 2 s, except in the control spectra for which a 12 s delay was used to ensure full water relaxation. To account for the reduction of steady-state water magnetization by a factor of ~ 0.7, the reported k_{ex} values were scaled by 1.4-fold.

Results and discussion

Detection of serine and threonine hydroxyl signals

The use of selective isotopic labeling and long-range ^{13}C-HSQC experiments provides a simple route for detecting and unambiguously assigning slowly exchanging hydroxyl

proton signals. In a conventional gradient ^{13}C-HSQC spectrum recorded with a standard INEPT "1/4J" delay of 1.7 ms, the expected signals from directly-bonded ^{1}H–^{13}C groups were readily observed in samples of ^{13}C/^{15}N-serine or -threonine labeled BcX. In contrast, spectra recorded with ∼11 ms delays yielded additional weak crosspeaks due to long-range $^3J_{C–OH}$ couplings between the hydroxyl ^{1}H$^{\gamma 1}$ and methyl ^{13}C$^{\gamma 2}$ pairs of three threonines (Fig. 2) and the ^{1}H$^\gamma$ and ^{13}C$^\alpha$ pairs of two serines (Fig. 3). Importantly, these signals were apparent singlets with or without ^{13}C- or ^{15}N-decoupling during acquisition, thus confirming that they indeed corresponded to oxygen-bonded protons. By alignment with the reference one-bond spectra, the hydroxyls were readily assigned to Thr72, Thr145, Thr171, Ser130, and Ser176.

Several details of this strategy, which has been demonstrated for tyrosines (Baturin et al. 2011) and should also work with cysteines, are worth comment. In addition to providing immediate amino acid-specific assignments, selective ^{13}C- or ^{13}C/^{15}N-labeling is advantageous for several reasons. The multitude of potential one-, two- and three-bond ^{1}H–^{13}C correlations present in the long-range ^{13}C-HSQC spectrum of a uniformly enriched protein could easily obscure the desired hydroxyl signal. Unlike the generally downfield shifted phenolic protons of tyrosines, these threonine and serine OH signals fall across the spectral envelope typical of many amide, aromatic, and aliphatic protons. Also, even if clearly identified as an OH signal (i.e., by comparing spectra recorded ±^{15}N/^{13}C decoupling during acquisition or in H$_2$O vs D$_2$O buffer), chemical shift degeneracy along the ^{13}C dimension of a

long-range ^{13}C-HSQC spectrum recorded with a uniformly enriched protein might preclude an unambiguous assignment. In contrast, these complications are significantly reduced by using selective ^{13}C-labeling, thus enabling the confident detection and assignment of signals from only serine or threonine hydroxyls. Of course, labeling with ^{13}C$^\alpha$-Ser or ^{13}C$^{\gamma 2}$-Thr would provide even further spectral simplification, albeit at the cost of obtaining these compounds via synthetic or biosynthetic routes (Velyvis et al. 2012). Also, various deuteration approaches can be envisioned. However, the uniformly ^{13}C/^{15}N-enriched amino acids purchased for this study were obtained from an algal lysate and thus relatively inexpensive. This labeling scheme also facilitated residue-specific assignments using amide ^{15}N-resolved ^{13}C-TOCSY approaches. On the other hand, a disadvantage of this scheme is peak broadening in ^{13}C-HSQC spectra due to ^{13}C–^{13}C couplings. Although the latter can be avoided with a constant-time pulse sequence (Supplemental Figs. S6 and S7), the required ∼26 ms delay resulted in substantial signal loss with the BcX samples (not shown). Fortunately, in the case of threonine, the ^{13}C$^{\gamma 2}$ resonate over 40 ppm upfield from the ^{13}C$^{\alpha/\beta}$, thus allowing decoupling in t_1 with a selective ^{13}C inversion pulse applied at 70 ppm to sharpen the detected ^{13}C$^{\gamma 2}$–H$^{\gamma 1}$ peaks (Supplemental Fig. S8).

Even with selective labeling, the hydroxyl protons in BcX have chemical shifts ranging from 2.9 to 7.8 ppm and thus potentially overlap resonances from other serine and threonine protons (e.g., Ser176 in Fig. 4). Therefore, it was also critical to use empirically optimized INEPT "1/4J" delays of 10.5 ms for serine and 11.4 ms for threonine in
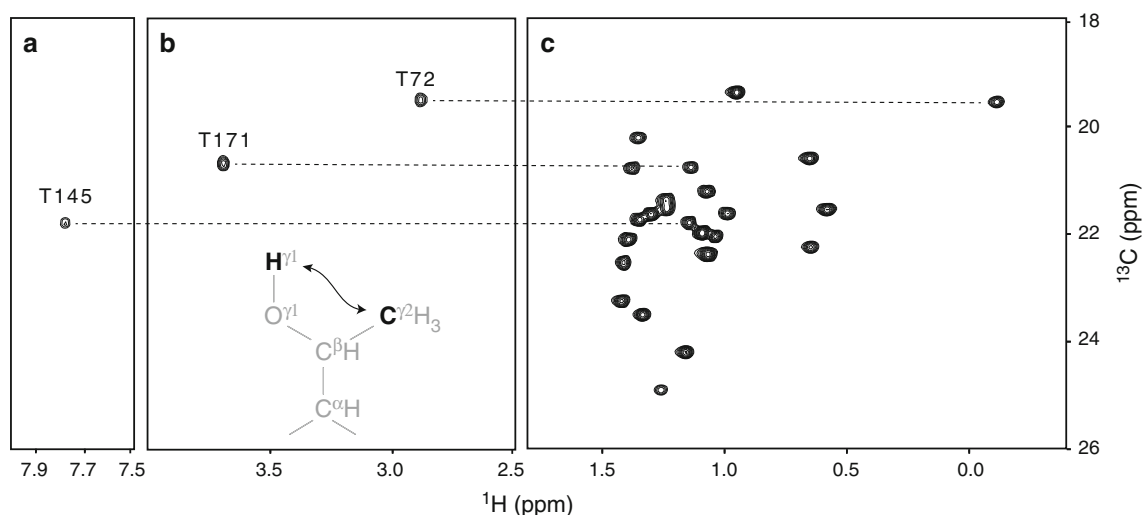

Fig. 2 a, b Signals from three hydroxyl ^{1}H$^{\gamma 1}$ nuclei in selectively ^{13}C/^{15}N-threonine labeled BcX were detected in a long-range ^{13}C$^\beta$-decoupled ^{13}C-HSQC spectrum that exploits a weak $^3J_{C–OH}$ coupling to the methyl ^{13}C$^{\gamma 2}$. **c** The signals were then assigned by alignment with a one-bond constant-time ^{13}C-HSQC spectrum (contoured ∼×2

higher than **a, b**). To detect the $^3J_{C–OH}$ couplings, while also minimizing signals from directly bonded ^{1}H–^{13}C groups, an INEPT "1/4J" delay of 11.4 ms was used for the long-range experiment (Supplemental Figs. S7 and S8)
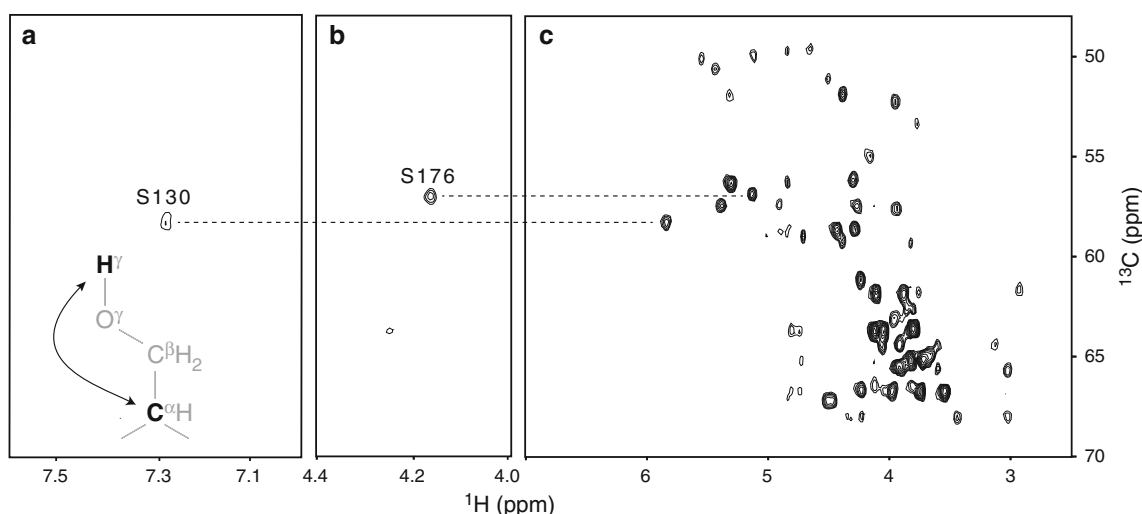
Fig. 3 Signals from two hydroxyl $^1H^\gamma$ nuclei in selectively $^{13}C/^{15}N$-serine labeled BcX were detected in a **a**, **b** long-range ^{13}C-HSQC spectrum that exploits a weak $^3J_{C-OH}$ coupling to the $^{13}C^\alpha$, and then assigned by aligning to a **c** one-bond ^{13}C-HSQC spectrum (contoured ~×2 higher than **a**, **b**). An INEPT "1/4J" delay of 10.5 ms was used for the long-range experiment in order to also minimize signals from

directly bonded $^{13}C-^1H$ groups (Supplemental Fig. S6). Note that Ser176 $^1H^\gamma$ has a chemical shift of 4.16 ppm, which falls within the range for most serine $^1H^\alpha$ and $^1H^\beta$ nuclei. Thus, good suppression of the one-bond couplings, as seen in **b**, was important for detecting this signal

order to minimize signals from directly bonded $^{13}C-^1H$ pairs (i.e., nulls occurring at $n/\{2^1J_{CH}\}$) while favouring long-range couplings. Although the choice of these timings was best for BcX due to a balance of one-bond signal suppression and relaxation versus transfer efficiency for detecting long-range hydroxyl couplings, OH signals were still observed with delays spanning 4 to 32 ms. Parenthetically, another advantage of selective isotopic labeling for the simple long-range ^{13}C-HSQC experiment lies with the difficulty in efficiently suppressing the signals from all $^{13}C-^1H$ pairs in a uniformly labeled protein sample due to the range of possible $^1J_{CH}$ couplings.

All five hydroxyls detected in the long-range ^{13}C-HSQC spectra are hydrogen bonded and either partially (Thr145) or completely solvent inaccessible in the static X-ray crystal structure of BcX. This, of course, is expected as these hydroxyls must be well protected from HX in order to be observed via this NMR approach. Of the 18 serines and 25 threonines in BcX, several additional residues, including Thr33, Thr67, Thr110, Ser100, and Ser180, are also fully buried and hydrogen bonded, and thus likely yield the remaining unassigned OH peaks in the $^{13}C/^{15}N$-filtered spectrum of Fig. 1b. Accordingly, the absence of any corresponding signals in a long-range ^{13}C-HSQC spectrum is somewhat surprising. Note that care was taken to limit the adverse effects of hydrogen exchange. In particular, the water magnetization was minimally perturbed through use of gradients, rather than selective saturation, and returned
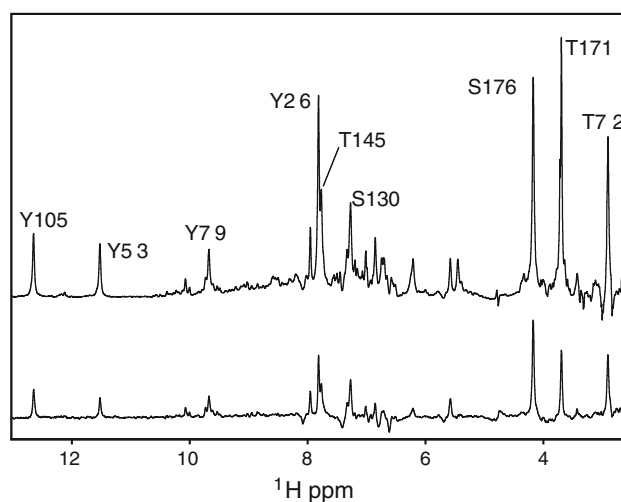

Fig. 4 The $^3J_{C-OH}$ couplings for the hydroxyl protons in uniformly $^{13}C/^{15}N$-labeled BcX were measured using a quantitative spin-echo difference experiment with a $^{13}C/^{15}N$-filtered readout. Shown are the reference (*top*) and difference (*lower*) spectra recorded with $\Delta = 21$ ms in the pulse sequence of Supplemental Fig. S9. The signals from Tyr26 and Thr145 were deconvoluted using Topspin. In addition to the results given in the text for the serines and threonines, apparent $|^3J_{C\varepsilon-H\eta}|$ values were also fit for Tyr105 (7.3 Hz), Tyr53 (6.6 Hz), Tyr79 (7.0 Hz), and Tyr26 (5.6 Hz). As reported previously (Baturin et al. 2011), $|^2J_{C\zeta-H\eta}|$ are small for tyrosines. Also, due to slow ring flipping and slow rotation about the $C^\zeta-O^\eta$ bond, the hydroxyl $^1H^\eta$ of Tyr79 is constrained by hydrogen bonding to a trans conformation relative to the coupled $^{13}C^\varepsilon$. The same holds for Tyr105. In contrast, the aromatic rings of Tyr26 and Tyr53 flip rapidly, giving averaged chemical shifts and, hence, $^3J_{C\varepsilon-H\eta}$ for their two $^{13}C^\varepsilon$ nuclei

to the +z-axis at the end of the ^{13}C-HSQC pulse sequences (Grzesiek and Bax 1993). One possible explanation is that some of these serine and threonine residues may have conformationally-restricted hydroxyls with a gauche $C^{\alpha/\gamma2}$–C^{β}–$O^{\gamma/\gamma1}$–$H^{\gamma/\gamma1}$ dihedral angle and thus relatively small $^{3}J_{C\alpha-H\gamma}$ and $^{3}J_{C\gamma2-H\gamma1}$ couplings, respectively (see below). Alternatively, the hydroxyls may be exchanging slowly enough to be detected in the 1D spectrum (i.e., $k_{ex} < {}^{1}J_{XH}$ ~100 s^{-1} for filtering ^{1}H–^{13}C and ^{1}H–^{15}N signals), yet fast enough ($k_{ex} > {}^{3}J_{CH}$ ~10 s^{-1}) to impair polarization transfer during the INEPT periods of the long-range ^{13}C-HSQC pulse sequences (Henry and Sykes 1990; Segawa et al. 2008).

A complementary approach to detecting slowly exchanging serine and threonine hydroxyls is to use a ^{13}C/^{15}N-filtered/edited HSQC-NOESY experiment (Ikura and Bax 1992; Zwahlen et al. 1997). Although typically recorded to detect *inter*molecular NOEs within a complex of isotopically labeled and unlabeled species, *intra*molecular NOEs will also be observed between oxygen-bonded and ^{13}C/^{15}N-bonded protons within a single uniformly labeled protein. Indeed many such NOEs can be detected for the slowly exchanging serine, threonine, and tyrosine hydroxyls in BcX (Baturin et al. 2011 and not shown). However, their unambiguous assignment proved very difficult due to potential chemical shift degeneracies. This precluded the confident identification of the remaining unassigned OH peaks in the ^{13}C/^{15}N-filtered spectrum of Fig. 1b.

Coupling constant measurements

It is notable that potential signals from $^{2}J_{CH}$ hydroxyl proton couplings with the ^{13}C$^{\beta}$ of either amino acid were not detected, nor were those from $^{3}J_{C-OH}$ couplings between the ^{1}H$^{\gamma1}$ and ^{13}C$^{\alpha}$ pairs of the threonines. For simple alcohols, $^{2}J_{C-OH}$ couplings of −2 to −3 Hz and dihedral angle-dependent $^{3}J_{C-OH}$ couplings of 2–9 Hz (assumed positive) have been reported (Hansen 1981; Borisov et al. 1998). Thus, the absence of these additional signals likely reflects weak, averaged scalar interactions, for which detection is limited by the relaxation behaviour of this 20 kDa protein.

The expected dihedral angle-dependence of the $^{3}J_{C-OH}$ couplings can also provide structural insights into the hydroxyl conformations. Therefore, we used a quantitative spin-echo difference experiment (Blake et al. 1992) combined with ^{13}C/^{15}N-filtration to measure the coupling constants for the five detected hydroxyls (Fig. 4). This yielded $|^{3}J_{C\alpha-H\gamma}|$ values of 6.9 Hz for Ser130 and 7.3 Hz for Ser176. For the threonines, $|^{3}J_{C\gamma2-H\gamma1}|$ values of 6.8 Hz for Thr72, 5.9 Hz for Thr145, and 5.4 Hz for Thr171 were measured. The fitting errors were estimated to be

±0.5 Hz, and additional possible couplings were assumed to be negligible due to the absence of corresponding signals in long-range ^{13}C-HSQC spectra. Although the Karplus equation for such $^{3}J_{C-OH}$ couplings has not been parameterized, the measured values suggest that all five hydroxyl protons are at least moderately restrained within BcX and predominantly in trans conformations relative to the coupled ^{13}C nucleus. Parenthetically, for each threonine with a trans $C^{\gamma2}$–C^{β}–$O^{\gamma1}$–$H^{\gamma1}$ dihedral angle, the corresponding C^{α}–C^{β}–$O^{\gamma1}$–$H^{\gamma1}$ would be in the gauche conformation. The latter would likely have a relatively small $^{3}J_{C\alpha-H\gamma1}$, thus explaining the lack of $^{13}C^{\alpha}$–$^{1}H^{\gamma1}$ crosspeaks for the three threonines detected in long-range ^{13}C-HSQC spectra. By way of comparison, in a long-range ^{13}C-HMQC spectrum of a CAP-Gly domain, a slowly exchanging threonine H$^{\gamma1}$ with an unusual shift of
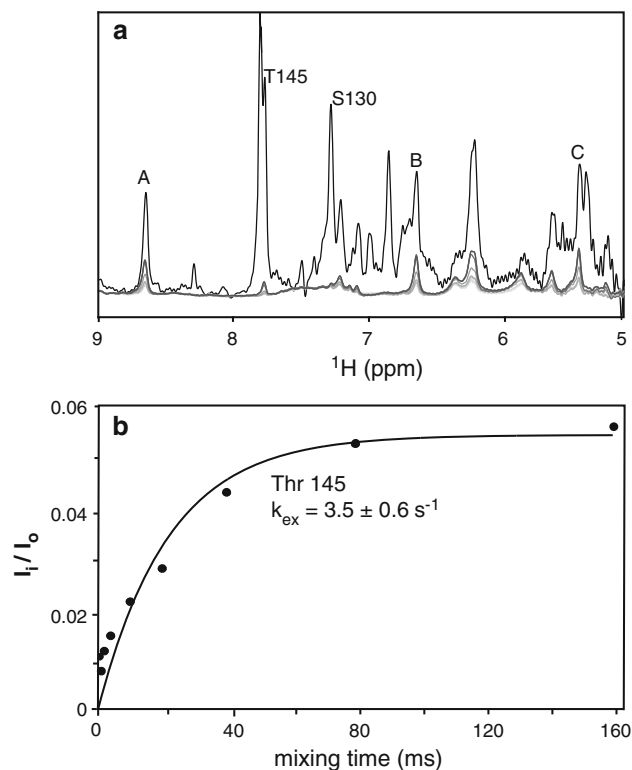

Fig. 5 The hydroxyl HX rates were measured at pH 6 and 25 °C using a CLEANEX-PM experiment with a ^{13}C/^{15}N-filtered readout. **a** Overlaid spectra with mixing times of 0.42, 0.84, 2, 4, 10, 20, 40, 80, 150 ms (*light grey* to *dark grey*) are shown along with a normalized reference spectrum (*black*). **b** The build-up exchange curve of Thr145 was fit to yield $k_{ex} = 3.5 \pm 0.6$ s^{-1} and $R_{app} = 43 \pm 10$ s^{-1}. Errors were estimated via a Monte Carlo approach. Note that Tyr26 does not show detectable exchange, and the reference signal intensity for the adjacent Thr145 was deconvoluted using Topspin. Several additional unassigned hydroxyls showed more rapid HX (*A*: 60 ± 20 s^{-1}; *B*: 70 ± 20 s^{-1}; and *C*: 110 ± 30 s^{-1}), which likely precluded their detection and assignment in long-range ^{13}C-HSQC spectra. The pulse sequence is summarized in Supplemental Fig. S10

−0.97 ppm showed a strong correlation to its $^{13}C^{\alpha}$ and a weak correlation to its $^{13}C^{\gamma 2}$ (Plevin et al. 2008). This threonine participates in an OH/π interaction with an adjacent phenylalanine ring, and indeed has a trans C^{α}–C^{β}–$O^{\gamma 1}$–$H^{\gamma 1}$ dihedral angle.

Hydrogen exchange kinetics

Serine and threonine hydroxyls undergo both specific and general acid- and base-catalyzed HX. Accordingly, long-range ^{13}C-HSQC spectra were recorded for the $^{13}C/^{15}N$-threonine labeled BcX sample at pH values ranging from 4 to 8 and temperatures from 5 to 25 °C. However, no additional hydroxyl signals were detected beyond those found initially at pH 6. This is consistent with the observation that serines and threonines in model peptides exchange most slowly at a pH_{min} of ~ 6.5 (Liepinsh et al. 1992; Liepinsh and Otting 1996).

To measure the HX kinetics of the BcX serine and threonine residues, a CLEANEX-PM experiment (Hwang et al. 1997) with $^{13}C/^{15}N$-filtered detection was implemented. As shown in Fig. 5, a reliable transfer curve was measurable for Thr145, yielding a fit exchange rate constant k_{ex} of 3.5 ± 0.6 s^{-1}. Based on the data of Liepinsh and Otting (Liepinsh et al. 1992), a reference $k_{ex} \sim 500$ s^{-1} can be estimated for a serine or threonine in a random coil peptide under similar experimental conditions. Thus, the HX rate of Thr145 is retarded by ~ 150-fold due to its structural and electrostatic environment in BcX. Although Ser130 appeared to be exchanging, overlap with neighbouring peaks in combination with low signal intensity made quantitation unreliable. In contrast, CLEANEX transfer was not detected for Thr72, Thr171 and Ser176. Thus, these residues likely have $k_{ex} < 1$ s^{-1} and protection factors > 500. Consistent with these relative rate HX rate constants, the latter three residues yielded stronger
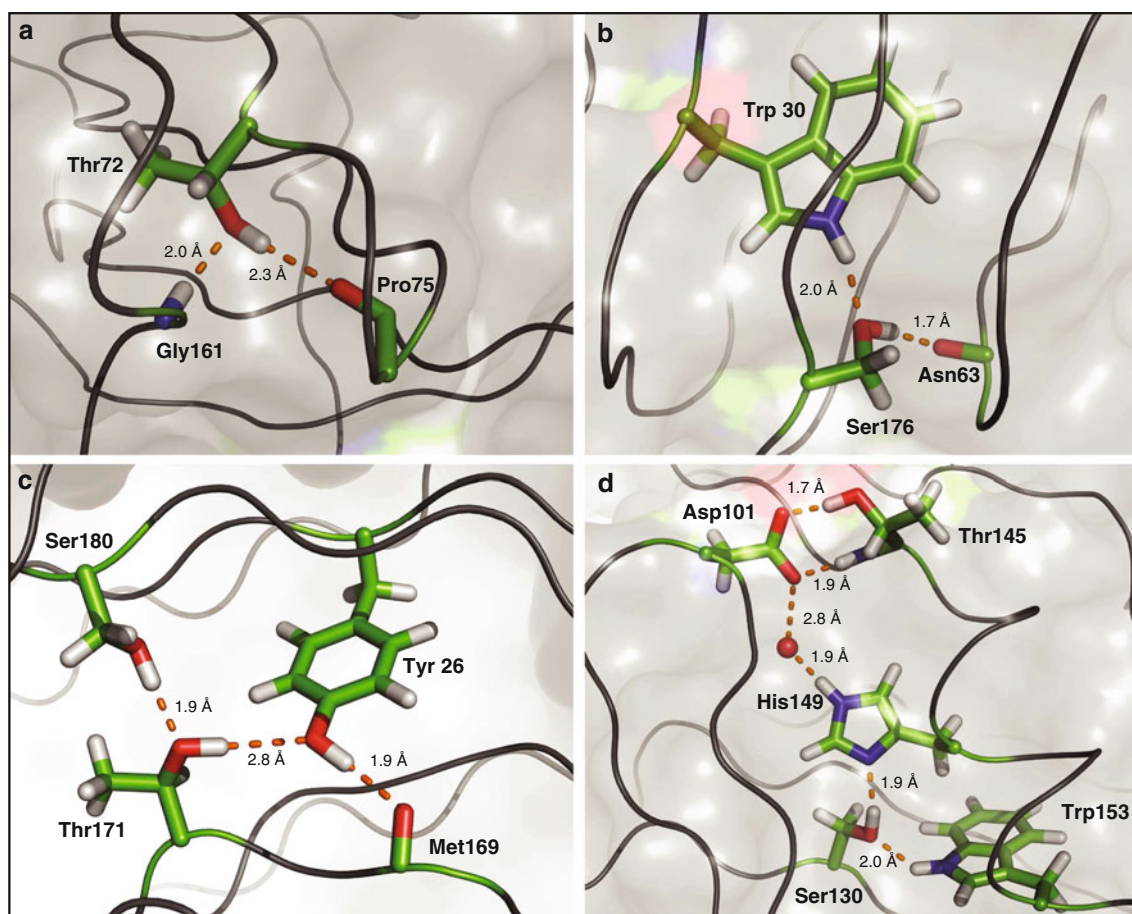

Fig. 6 NMR spectroscopy provides confirmatory insights into the structural features of several BcX serine and threonine hydroxyl protons determined previously by X-ray crystallography. Both **a** Thr72 and **b** Ser176 donate a hydrogen bond to a carbonyl oxygen and accept one from an amide or indole, respectively. **c** Thr171 is a weak hydrogen bond donor to Tyr26 and a strong acceptor for Ser180.

d Thr145 and Ser130 participate in an extensive hydrogen-bonding network also involving a charged aspartate, a buried neutral histidine, and an internal water. The program Reduce (Word et al. 1999) was used to add hydrogens to the protein coordinate file 1XNB.pdb (oxygen, *red*; nitrogen, *blue*; carbon, *green*; hydrogen, *grey*). Hydrogen bonds are indicated with *yellow dashes*

hydroxyl crosspeaks in long-range ^{13}C-HSQC spectra than did Thr145 and Ser130 (Figs. 2, 3). Conversely, several additional unassigned hydroxyls showed more rapid HX (60–110 s^{-1}; Fig. 4), which likely precluded their detection and assignment in long-range ^{13}C-HSQC spectra. Hydroxyl HX rate constants of a similar magnitude have also been measured recently using an elegant approach that exploits highly specific ^{13}C/^{2}H serine and threonine labeling along with deuterium isotope shifts (Takeda et al. 2011).

Structural insights

By combining NMR spectroscopic and X-ray crystallographic data, insights into the structural features of several hydroxyl in BcX can be obtained (Fig. 6). Based upon their relative positions in the X-ray crystallographic structure of BcX, it is very reasonable to propose that the sidechains of Thr72 and Ser176 both accept a hydrogen bond from a neighboring amide or indole, respectively, and donate a hydrogen bond to a carbonyl oxygen. This proposal is supported by the observed protection of these hydroxyls from rapid HX, and by coupling constant measurements, indicating that each is restrained in a trans $C^{\alpha/\gamma2}$–C^{β}–$O^{\gamma1}$–$H^{\gamma/\gamma1}$ conformation.

In a cluster of buried polar groups, Thr171 bridges Ser180 and Tyr26. The $O^{\gamma1}$ threonine appears positioned to both accept a hydrogen bond from the O^{γ}H of Ser180, and donate one to the phenol of Tyr26, which in turn donates a hydrogen bond to carbonyl of Met169. Although this is consistent with $^3J_{C–OH}$ measurements, indicating a trans $C^{\gamma2}$–C^{β}–$O^{\gamma1}$–$H^{\gamma1}$ dihedral angle for Thr171, the hydrogen bond to Tyr26 seems rather long in the crystal structure of BcX. Thus, it is somewhat surprising that the hydroxyl proton of Thr171 is well protected from HX, especially since that of Ser180 was not detected in long-range ^{13}C-HSQC despite an apparently strong interaction with this threonine. This highlights the difficulty in inferring such energetic and dynamic details from static crystal structures.

Thr145 and Ser130 are involved in a fascinating network of buried polar groups (Plesniak et al. 1996a; Joshi et al. 1997). Thr145 must donate a hydrogen bond to the negatively-charged carboxylate of Asp101, which is also linked via a bound water to the $N^{\epsilon2}$H of neutral His149. On the opposite side of the imidazole ring, Ser130 appears to donates its O^{γ}H to the $N^{\delta1}$ of this histidine, while accepting a hydrogen bond from the indole of Trp153. In this proposed arrangement, both Thr145 and Ser130 have trans $C^{\alpha/\gamma2}$–C^{β}–$O^{\gamma1}$–$H^{\gamma/\gamma1}$ conformations that are consistent with their measured $^3J_{C–OH}$ couplings. Although the hydroxyl $H^{\gamma1}$ of Thr145 is partially solvent exposed in the BcX crystal structure, it is still well protected from HX due to these presumably strong interactions.

It is notable that the five hydroxyl protons in detected BcX have chemical shifts ranging from 2.9 to 7.8 ppm (Fig. 1), and thus differ substantially from the average values of 5.47 ± 1.1 ppm (serine $^1H^{\gamma}$) and 5.47 ± 1.1 ppm (threonine $^1H^{\gamma1}$) reported in the BioMagResBank (Ulrich et al. 2008). Inspection of the static crystal structure of BcX does not provide any simple consistent explanation for this chemical shift variation in terms of hydrogen bonding or proximity to aromatic rings (Fig. 6). One exception to this statement is that, of the five serines and threonines characterized in this study, only Thr145 is involved in an ionic hydrogen bond to negatively-charged acceptor (Asp101), and its $H^{\gamma1}$ has the most downfield shifted signal at 7.8 ppm.

Summary

The direct characterization of protein hydroxyl protons is usually a difficult challenge for structural biologists. Using a combination of selective isotope labeling along with various isotope filtering and editing strategies, we have detected and assigned the ^{1}H signals from five slowly exchanging serine and threonine hydroxyls in BcX. These approaches were also exploited to measure $^3J_{C–OH}$ couplings and HX kinetics and thereby gain structural and dynamic insights into the local environments of these residues within this model protein. These methods should prove useful for further studies of functionally important hydroxyls in a variety of proteins and protein complexes.

Supplemental data

Supplemental data showing assignment spectra and the NMR pulse sequences used in this study can be found in the online version.

References

Agarwal V, Linser R, Fink U, Faelber K, Reif B (2010) Identification of hydroxyl protons, determination of their exchange dynamics, and characterization of hydrogen bonding in a microcrystallin protein. J Am Chem Soc 132:3187–3195

Baba T, Ara T, Hasegawa M, Takai Y, Okumura Y, Baba M, Datsenko KA, Tomita M, Wanner BL, Mori H (2006)

Construction of *Escherichia coli* K-12 in-frame, single-gene knockout mutants: the Keio collection. Mol Syst Biol 2:2006

Baturin SJ, Okon M, McIntosh LP (2011) Structure, dynamics, and ionization equilibria of the tyrosine residues in *Bacillus circulans* xylanase. J Biomol NMR 51:379–394

Blake PR, Lee B, Summers MF, Adams MWW, Park JB, Zhou ZH, Bax A (1992) Quantitative measurement of small through-hydrogen-bond and through-space $^{1}H–^{113}Cd$ and $^{1}H–^{199}Hg$ J-couplings in metal-substituted rubredoxin from *Pyrococcus furiosus*. J Biomol NMR 2:527–533

Borisov EV, Zhang W, Bolvig S, Hansen PE (1998) $^{n}J(^{13}C, O^{1}H)$ coupling constants of intramolecularly hydrogen-bonded compounds. Magn Reson Chem 36:S104–S110

Breeze AL (2000) Isotope-filtered NMR methods for the study of biomolecular structure and interactions. Prog Nucl Magn Reson Spectrosc 36(4):323–372

Clark AJ (1963) Genetic analysis of a "double male" strain of *Escherichia coli* K-12. Genetics 48:105–120

Connelly GP, Withers SG, McIntosh LP (2000) Analysis of the dynamic properties of *Bacillus circulans* xylanase upon formation of a covalent glycosyl-enzyme intermediate. Protein Sci 9:512–5242

Creighton TE (2010) The biophysical chemistry of nuclei acids and proteins. Helvetian Press, NY

Delaglio F, Grzesiek S, Vuister GW, Zhu G, Pfeifer J, Bax A (1995) NNMpipe—a multidimensional spectral processing system based on Unix pipes. J Biomol NMR 6(3):277–293

Goddard TD, Kneeler DG (1999) Sparky 3, 3rd edn. University of California, San Francisco, CA

Grzesiek S, Bax A (1993) The importance of not saturating H_2O in protein NMR—application to sensitivity enhancement and NOE measurements. J Am Chem Soc 115:12593–12594

Hansen PE (1981) Carbon–hydrogen spin–spin coupling constants. Prog Nucl Magn Reson Spectrosc 14:175–295

Henry GD, Sykes BD (1990) Hydrogen exchange kinetics in a membrane protein determined by ^{15}N NMR spectroscopy: use of the INEPT experiment to follow individual amides in detergent-solubilized M13 coat protein. Biochemistry 29:6303–6313

Ho BK, Agard DA (2008) Identification of new, well-populated amino-acid sidechain rotamers involving hydroxyl-hydrogen atoms and sulfhydryl-hydrogen atoms. BMC Struct Biol 8:41

Hwang TL, Mori S, Shaka AJ, vanZijl PCM (1997) Application of phase-modulated CLEAN chemical EXchange spectroscopy (CLEANEX-PM) to detect water-protein proton exchange and intermolecular NOEs. J Am Chem Soc 119:6203–6204

Ikura M, Bax A (1992) Isotope-filtered 2D NMR of a protein peptide complex—study of a skeletal-muscle myosin light chain kinase fragment bound to calmodulin. J Am Chem Soc 114:2433–2440

Iwahara J, Wojciak JM, Clubb RT (2001) Improved NMR spectra of a protein-DNA complex through rational mutagenesis and the application of a sensitivity optimized isotope-filtered NOESY experiment. J Biomol NMR 19:231–241

Joshi MD, Hedberg A, McIntosh LP (1997) Complete measurement of the pKa values of the carboxyl and imidazole groups in *Bacillus circulans* xylanase. Protein Sci 6:2667–2670

Joshi MD, Sidhu G, Nielsen JE, Brayer GD, Withers SG, McIntosh LP (2001) Dissecting the electrostatic interactions and pH-dependent activity of a family 11 glycosidase. Biochemistry 40:10115–10139

Knauf MA, Lohr F, Curley GP, O'Farrell P, Mayhew SG, Muller F, Ruterjans H (1993) Homonuclear and heteronuclear NMR studies of oxidized *Desulfovibrio vulgaris* flavodoxin. Sequential assignments and identification of secondary structure elements. Eur J Biochem 213:167–184

Kossiakoff AA, Shpungin J, Sintchak MD (1990) Hydroxyl hydrogen conformations in trypsin determined by the neutron-diffraction solvent difference map method—relative importance of steric

and electrostatic factors in defining hydrogen-bonding geometries. Proc Natl Acad Sci USA 87:4468–4472

Liepinsh E, Otting G (1996) Proton exchange rates from amino acid side chains—implications for image contrast. Magn Reson Med 35:30–42

Liepinsh E, Otting G, Wuthrich K (1992) NMR spectroscopy of hydroxyl protons in aqueous solutions of peptides and proteins. J Biomol NMR 2:447–465

Lohr F, Mayhew SG, Ruterjans H (2000) Detection of scalar couplings across NH···OP and OH···OP hydrogen bonds in a flavoprotein. J Am Chem Soc 122:9289–9295

McIntosh LP, Naito D, Baturin SJ, Okon M, Joshi MD, Nielsen JE (2011) Dissecting electrostatic interactions in *Bacillus circulans* xylanase through NMR-monitored pH titrations. J Biomol NMR 51:5–19

Muchmore DC, McIntosh LP, Russell CB, Anderson DE, Dahlquist FW (1989) Expression and ^{15}N labeling of proteins for proton and ^{15}N NMR. Methods Enzymol 177:44–73

Ogura K, Terasawa H, Inagaki F (1996) An improved double-tuned and isotope-filtered pulse scheme based on a pulsed field gradient and a wide-band inversion shaped pulse. J Biomol NMR 8:492–498

Peelen S, Vervoort J (1994) Two-dimensional NMR studies of the flavin binding site of *Desulfovibrio vulgaris* flavodoxin in its three redox states. Arch Biochem Biophys 314:291–300

Piotto M, Saudek V, Sklenar V (1992) Gradient-tailored excitation for single-quantum NMR-spectroscopy of aqueous solutions. J Biomol NMR 2:661–665

Plesniak LA, Connelly GP, Wakarchuk WW, McIntosh LP (1996a) Characterization of a buried neutral histidine residue in *Bacillus circulans* xylanase: NMR assignments, pH titration, and hydrogen exchange. Protein Sci 5(11):2319–2328

Plesniak LA, Wakarchuk WW, McIntosh LP (1996b) Secondary structure and NMR assignments of *Bacillus circulans* xylanase. Protein Sci 5(6):1118–1135

Plevin MJ, Hayashi I, Ikura M (2008) Characterization of a conserved "threonine clasp" in CAP-Gly domains: role of a functionally critical OH/π interaction in protein recognition. J Am Chem Soc 130:14918–14919

Segawa T, Kateb F, Duna L, Bodnhausen G, Pelupessy P (2008) Exchange rate constants of invisible proteins in proteins determined by NMR spectroscopy. ChemBioChem 9:537–542

Sung WL, Luk CK, Zahab DM, Wakarchuk W (1993) Overexpression and purification of the *Bacillus subtilis* and *Bacillus circulans* xylanases in *Escherichia coli*. Protein Expr Purif 4:200–216

Takeda M, Jee J, Ono AM, Terauchi T, Kainosho M (2011) Hydrogen exchange study on the hydroxyl groups of serine and threonine residues in proteins and structure refinement using NOE restraints with polar side-chain groups. J Am Chem Soc 133:17420–17427

Ulrich EL, Akutsu H, Doreleijers JF, Harano Y, Ioannidis YE, Lin J, Livny M, Mading S, Maziuk D, Miller Z, Nakatani E, Schulte CF, Tolmie DE, Wenger RK, Yao HY, Markley JL (2008) BioMagResBank. Nucleic Acids Res 36:D402–D408

Velyvis A, Ruschak AM, Kay LE (2012) An economical method for production of ^{2}H, $^{13}CH_3$-threonine for solution NMR studies of large protein complexes: application to the 670 kDa proteasome. PLoS ONE 7(9):e43725

Waugh DS (1996) Genetic tools for selective labeling of proteins with α-^{15}N-amino acids. J Biomol NMR 8:184–192

Word JM, Lovell SC, Richardson JS, Richardson DC (1999) Asparagine and glutamine: using hydrogen atom contacts in the choice of side-chain amide orientation. J Mol Biol 285:1735–1747

Zwahlen C, Legault P, Vincent SJF, Greenblatt J, Konrat R, Kay LE (1997) Methods for measurement of intermolecular NOEs by multinuclear NMR spectroscopy: application to a bacteriophage lambda N-peptide/boxB RNA complex. J Am Chem Soc 119:6711–6721